THE FASEB JOURNAL • RESEARCH • www.fasebj.org

# Cilostazol ameliorates ischemia/reperfusion-induced tight junction disruption in brain endothelial cells by inhibiting endoplasmic reticulum stress

**Ding Nan, Haiqiang Jin, Jianwen Deng, Weiwei Yu, Ran Liu, Weiping Sun, and Yining Huang[1]**
Department of Neurology, Peking University First Hospital, Beijing, China

**ABSTRACT: Endoplasmic reticulum (ER) stress is essential for brain ischemia/reperfusion (I/R) injury. However, whether it contributes to I/R-induced blood-brain barrier (BBB) injury remains unclear. cilostazol exerts protective effects toward I/R-induced BBB injury, with unclear mechanisms. This study explored the potential role of ER stress in I/R-induced endothelial cell damage and determined whether the therapeutic potential of cilostazol, with respect to I/R-induced endothelial cell damage, is related to inhibition of ER stress. We found that exposing brain endothelial cells (bEnd.3) to oxygen-glucose deprivation/reoxygenation (OGD/R) significantly activated ER stress and diminished the barrier function of cell monolayers; treatment with the ER stress inhibitor 4-phenylbutyric acid (4-PBA) or cilostazol prevented OGD/R-induced ER stress and preserved barrier function. Furthermore, OGD/R induced the expression and secretion of matrix metalloproteinase-9 and nuclear translocation of phosphorylated NF-κB. These changes were partially reversed by 4-PBA or cilostazol treatment. *In vivo*, 4-PBA or cilostazol significantly attenuated I/R-induced ER stress and ameliorated Evans blue leakage and tight junction loss. These results demonstrate that I/R-induced ER stress participates in BBB disruption. Targeting ER stress could be a useful strategy to protect the BBB from ischemic stroke, and cilostazol is a promising therapeutic agent for this process.—Nan, D., Jin, H., Deng, J., Yu, W., Liu, R., Sun, W., Huang, Y. Cilostazol ameliorates ischemia/reperfusion-induced tight junction disruption in brain endothelial cells by inhibiting endoplasmic reticulum stress. FASEB J. 33, 000–000 (2019). www.fasebj.org**

**KEY WORDS: Ischemia/reperfusion injury · blood-brain barrier disruption · endothelial cell · paracellular permeability**

Ischemic stroke is a common cause of death and disability worldwide and exerts a tremendous economic burden on society (1). Rapid recanalization is often chosen as a therapeutic strategy whenever conditions are favorable (2). However, restoring cerebral blood supply can instead result in reperfusion injury (3, 4). Blood-brain barrier (BBB) disruption after ischemia/reperfusion (I/R) is considered one of the main mechanisms of hemorrhagic transformation (HT) after ischemic stroke. However, the mechanism of I/R injury is still not clear, and effective methods for the prevention of cerebral I/R injury have not been established.

Recent studies have revealed that endoplasmic reticulum (ER) stress is an essential signaling event during neuronal injury after I/R (5). The ER is the earliest site to respond to cellular stress (6). Further, biologic stress can disturb the function of the ER and activate the ER stress response (6). Initially, ER stress leads to adaptations to the changing environment and the restoration of normal ER function (6). However, when severe or persistent ER stress cannot be corrected, cellular apoptosis is triggered (7). Cerebral ischemia was reported to disrupt ER function in neuronal cells, and ER stress was found to induce calcium overload (8), the cessation of protein synthesis (9), and apoptosis (10), which might ultimately lead to neuronal cell death. Although many studies on the effect of ER stress in neuronal cells exist, little attention has been paid to the effect of ER stress on endothelial cells and BBB disruption after I/R.

It was recently reported that cilostazol, an inhibitor of type III phosphodiesterase, not only is neuroprotective against ischemic stroke (11) but also has protective effects on vascular endothelial cells (12–14).

**ABBREVIATIONS:** 4-PBA, 4-phenylbutyric acid; ATF-6, activating transcription factor 6; BBB, blood-brain barrier; Bip, binding Ig protein; BMVEC, brain microvascular endothelial cell; CCK-8, Cell Counting Kit 8; EB, Evans blue; ECA, external carotid artery; ER, endoplasmic reticulum; HT, hemorrhagic transformation; I/R, ischemia/reperfusion; IRE1-α, inositol-requiring enzyme 1-α; LDH, lactate dehydrogenase; MMP-9, matrix metalloproteinase-9; OGD, oxygen-glucose deprivation; OGD/R, OGD/reoxygenation; PERK, protein kinase RNA-like ER kinase; TEER, transepithelial electrical resistance; TJ, tight junction; ZO-1, zonula occludens-1

[1] Correspondence: Peking University First Hospital, No.8 Xishiku St., Xicheng District, Beijing, 100034, PR China. E-mail: ynhuang@bjmu.edu.cn

doi: 10.1096/fj.201900326R
This article includes supplemental data. Please visit *http://www.fasebj.org* to obtain this information.

However, the molecular mechanisms associated with cilostazol are not completely understood.

In this study, we aimed to explore the role of ER stress in BBB disruption in the context of I/R injury, as well as its possible associated mechanisms, to uncover effective treatments for this process. Furthermore, in this study, we verified that cilostazol exerts its protective effects on BBB disruption after I/R injury by inhibiting ER stress.

## MATERIALS AND METHODS

### Cell culture and treatments

Immortalized brain microvascular endothelial cells (BMVECs) derived from mice (bEnd.3) were purchased from the American Type Culture Collection (ATCC; Manassas, VA, USA). Cells were cultured in 25-$cm^2$ culture flasks (for multiplying), 6-well plates (for Western blotting and RT-PCR), 24-well plates (for immunofluorescence staining), and 96-well plates (for cell viability and cytotoxicity assays). Transwell membrane inserts in 24-well plates [for the measurement of transepithelial electrical resistance (TEER) and paracellular permeability assays] were used at a seeding density of $5.0 \times 10^4$ to $5.0 \times 10^5$ cells/well. Cells were maintained in a humidified incubator (95% air/5% $CO_2$; Thermo Fisher Scientific, Waltham, MA, USA) with DMEM (Thermo Fisher Scientific) supplemented with 10% fetal bovine serum (Thermo Fisher Scientific), 100 U/ml penicillin, and streptomycin (Thermo Fisher Scientific) at 37°C. bEnd.3 cells were used between passages 29 and 39.

Cells were pretreated with the ER stress inhibitor 4-phenylbutyric acid (4-PBA; MilliporeSigma, Burlington, MA, USA) or cilostazol (Selleckchem, Houston, TX, USA) dissolved in DMSO (MilliporeSigma) 1 h before oxygen-glucose deprivation (OGD) and during OGD/reoxygenation (OGD/R).

### OGD/R

OGD/R was induced as follows. Confluent cells were washed twice with fresh medium, which was replaced with glucose-free DMEM pregassed with 95% $N_2$/5% $CO_2$ and then incubated with 95% $N_2$/5% $CO_2$ for 6 h. Cells were then reperfused by placing them in the fresh normal DMEM and were maintained in an incubator with 95% air/5% $CO_2$. Control cells were incubated with fresh normal medium for 6 h, reperfused, and maintained with normal medium with 95% air/5% $CO_2$ in a manner identical to that for OGD/R.

### Cell viability and cytotoxicity measurements

Cell viability was determined by adding Cell Counting Kit 8 (CCK-8) reagent (1:10 dilution in medium; Dojindo, Kumamoto, Japan) to cells after 6 h of OGD and 18 h of reperfusion. The optical density of the plates was measured as the absorbance at a wavelength of 450 nm using a microplate reader (Synergy 4, BioTek Instruments, Winooski, VT, USA), and cell viability was expressed as the percentage of optical density for cells exposed to OGD/R to that of control cells. Doses of 4-PBA and cilostazol were predetermined by testing serial doses in bEnd.3 cells exposed to OGD/R; CCK-8 assays showed that 100 mM of 4-PBA and 3 μM of cilostazol significantly improved cell viability after OGD/R.

To measure cell death and cell lysis, lactate dehydrogenase (LDH) activity in the cell culture medium was measured with LDH Cytotoxicity Assay Kit (Beyotime, Shanghai, China). The absorbance intensity of LDH activity was measured at 490 nm using a microplate reader, and cytotoxicity (%) was determined as the fold change relative to control cell viability.

### TEER

TEER was assessed to determine the integrity of brain endothelial monolayers using the TEER detection system EVOM2 (World Precision Instruments, Sarasota, FL, USA) with STX2 electrodes. In brief, bEnd.3 cells were seeded in Transwell inserts of 24-well plates at a density of $5 \times 10^4$/well and cultured until they reached confluence, replacing the culture medium every 2 d. Prior to use, the machine was calibrated; then, the longer electrode was placed to touch the bottom of the dish, whereas the shorter electrode was prevented from reaching the bottom of the insert. The readings were corrected using Transwell inserts with no cells (subtracted from each experimental measurement) and then standardized by the area of the culture inserts.

### Paracellular permeability assays

bEnd.3 cells were cultured on cell culture inserts at a density of $4 \times 10^4$. OGD/R was performed when cultured cells were confluent. After reoxygenation for 18 h, Na-F (1 mg/ml; Salibrobio, Beijing, China) was added into the upper compartment and then incubated for 30 min. The sample medium of the lower compartment was then removed and diluted 100-fold with PBS, and fluorescence intensity was measured at excitation and emission wavelengths of 485 and 525 nm, respectively, using a fluorescent reader (BioTek Instruments).

### Western blot analysis

Protein was isolated from cells, and a significant volume was loaded, electrophoresed, and transferred to PVDF membranes (MilliporeSigma). After blocking, membranes were incubated overnight with antibodies against claudin-5, zonula occludens-1 (ZO-1), (1:1000; Abcam, Cambridge, United Kingdom), occludin, activating transcription factor 6 (ATF-6; 1:1000; Proteintech, Chicago, IL, USA), p–inositol-requiring enzyme 1-α (IRE1-α; 1:1000; Thermo Fisher Scientific), binding Ig protein (Bip), IRE1-α, phosphorylated(p) protein kinase RNA like ER kinase (PERK), PERK, p-NF-κB, (1:1000; Cell Signaling Technology, Danvers, MA, USA), and β-actin (1:5000; ZSGB-Bio, Beijing, China). After a 1-h incubation with horseradish peroxidase–conjugated secondary antibodies (1:6000; ZSGB-Bio), protein bands were visualized using ECL (MilliporeSigma) with a detection system (GBOX-CHEMI-XT4, GENE, Hong Kong, China). Densities of each band were normalized to those of β-actin, whereas phosphorylated proteins were normalized to those of total proteins, using ImageJ software v.1.37 (National Institutes of Health, Bethesda, MD, USA).

### RNA isolation and RT-PCR

Total RNA was isolated using Trizol reagent (Thermo Fisher Scientific) and was reverse transcribed using reverse transcriptase (Thermo Fisher Scientific) to produce cDNA. The cDNA was mixed with Sybr Green Master Mix (Thermo Fisher Scientific) together with PCR primers, and RT-PCR was performed using 7500 (Thermo Fisher Scientific). PCR primers were as follows: mouse matrix metalloproteinase-9 (MMP-9) (5′-ACGACATAGACGGGCATCCA-3′ and 5′-GCTGTGGTTCAGTTGTGGTG-3′) and β-actin (5′-ACTATCGGCAATGAGCGGTTCC-3′ and 5′-AGCACTGTGTTGGCATAGAGGTC-3′). Relative fold changes were calculated by the $2^{-\Delta\Delta Ct}$ method.

### ELISA

After treatment, the culture medium of each group was collected and frozen at −80°C until analysis using an MMP-9 ELISA kit (EIAab, Wuhan, China). For this, 100 μl of sample or standard was added to each microplate well and then incubated for 2 h at 37°C. The liquid from each well was then removed, and then 100 μl of detection reagent A working solution was added to each well without washing, and samples were incubated for 1 h at 37°C. After washing, 100 μl of detection reagent B working solution was added and incubated for 1 h at 37°C. Next, after washing, 90 μl of substrate solution was added, and samples were incubated in the dark; 50 μl of stop solution was added 10–20 min later. The absorbance was measured at 450 nm using a microplate reader.

### Immunofluorescence staining

Cells were fixed with 4% paraformaldehyde and blocked in PBS containing 0.1% Triton X-100 and 5% goat serum for 1 h. Then, cells were incubated with primary antibodies against ZO-1 (1:50; Proteintech), occludin (1:50; Proteintech), and claudin-5 (1:100; Abcam) at 4°C overnight. Secondary antibodies conjugated with FITC (1:100; ZSGB-Bio) were then applied to cells for 1 h. Cells were mounted with mounting medium containing DAPI (ZSGB-Bio) after washing. Fluorescence images were obtained using a fluorescence microscope (Ti2E, Nikon, Tokyo, Japan).

### Rat cerebral I/R model

Male Sprague-Dawley rats weighing 300–320 g were used for this experiment, and the cerebral I/R model was generated. Briefly, after anesthetizing with pentobarbital at 50 mg/kg *via* intraperitoneal injection, rats were sterilized following skin preparation. A 2-cm-long incision was made in the middle of the neck, and the right common carotid artery, internal carotid artery, and external carotid artery (ECA) were gently separated. Then, the ECA was ligated and cut through. A silicon-coated 6–0 surgical monofilament nylon suture was inserted 17 ± 0.5 mm from the origin of the ECA into the internal carotid artery to reach the circle of Willis to occlude the origin of the right middle cerebral artery. After 2 h of occlusion, the suture was withdrawn, and reperfusion was initiated. Then, the incision was closed, and the animal was allowed to recover. A total of 50 male Sprague-Dawley rats were used in this study. Two of them were excluded because of death at the second day after surgery. Animals were randomly allocated to treatment groups, and the investigators performing surgeries and euthanizing animals had no knowledge of the experimental group to which an animal belonged. All experiments were performed according to the Guideline for the Care and Use of Experimental Animals of Peking University First Hospital (J201754).

Rats were randomly assigned to 4 experimental groups as follows: sham-treated, I/R, I/R + 4-PBA, and I/R + cilostazol. Cilostazol was suspended in 0.5% carboxymethyl cellulose sodium salt (Salibrobio) and administered orally for 3 d before ischemia. The other group received the same amount of vehicle for the same duration; the ER stress inhibitor 4-PBA (200 μM in 2 μl) was injected into the right cerebral ventricle (from the bregma: anterior–posterior, −0.8 mm; medial–lateral, 1.2 mm; dorsal–ventral, 4.0 mm) with a Microsyringe (Hamilton, Bonaduz, Switzerland) immediately after the onset of ischemia. The injection rate was 0.5 μl/min, and the cannula remained in place for 3 min after injection. The other group received the same amount of vehicle for the same duration. The signs of a successful surgery included the following: flexion or less grasping ability of the left foreleg and spontaneous circling or toppling to the left. Rats were evaluated for clinical signs of stroke and scored as follows: 0, no paralysis; 1, flexion of contralateral foreleg; 2, less grasping ability of the left foreleg when lifted up; 3, circling when pulled; 4, circling spontaneously; 5, disturbance of consciousness and death.

### Measurement of BBB disruption using Evans blue dye

The integrity of the BBB was examined using Evans blue (EB) dye extravasation. At 1 d after I/R, rats were injected *via* the tail vein with 2% EB (4 ml/kg; MilliporeSigma) and euthanized through an overdose of pentobarbital sodium 2 h later. Then, the rats were transcardially perfused with 0.9% NaCl until the outflow fluid from the right atrium was clear. Next, their brains were dissected, weighed, and incubated in formamide solution in a 37°C water bath. The EB that infiltrated into the brain tissue was then dissolved in the formamide solution. Next, 48 h later, the EB concentration in the formamide solution was measured using a microplate spectrophotometer (Synergy 4; BioTek Instruments) or perfused by saline followed by 4% paraformaldehyde. The brains were removed and cut into 20-μm-thick sections with a cryostat. The fluorescence of EB in spinal tissues was observed by confocal microscopy.

### Statistical analysis

All analyses were performed using SPSS 20.0 software (IBM SPSS, Chicago, IL, USA). Results are expressed as means ± SEM. We used a 1-way ANOVA followed by a *post hoc* Bonferroni multiple comparison test to compare the effects of each group if the data exhibited a normal distribution and homogeneity of variance. Otherwise, the differences were assessed by a nonparametric test. Values of $P < 0.05$ were considered statistically significant.

## RESULTS

### OGD/R-induced brain endothelial cell injury and tight junction disruption

To verify the effects of OGD/R on brain endothelial cells using an *in vitro* method of I/R (**Fig. 1*A***), cell viability and cytotoxicity were examined in bEnd.3 cells exposed to 18 h of reperfusion after 6 h of OGD. Cells exposed to OGD/R showed significant changes in cell viability compared with those maintained in control conditions (Fig. 1*B, C*). We further examined the effects of OGD/R on endothelial barrier function. OGD/R injury significantly decreased TEER and increased paracellular permeability compared with those in control conditions (Fig. 1*D, E*). Consistent with impaired paracellular permeability, levels of ZO-1 (0.69-fold change), occludin (0.64-fold change), and claudin-5 (0.60-fold change) were significantly decreased by OGD/R compared with those in control conditions (Fig. 1*F*). Additionally, immunofluorescence staining for ZO-1, occludin, and claudin-5 (green) showed reduced expression after OGD/R (Fig. 1*G*). These results suggest that the integrity of the endothelial cell barrier could be disrupted by OGD/R, partly *via* the down-regulation of tight junction (TJ) proteins, indicating that bEnd.3 cells exposed to 6 h of OGD and 18 h of reperfusion can serve as an *in vitro* I/R model for examining transient ischemic stroke–induced TJ injury in brain endothelial cells.

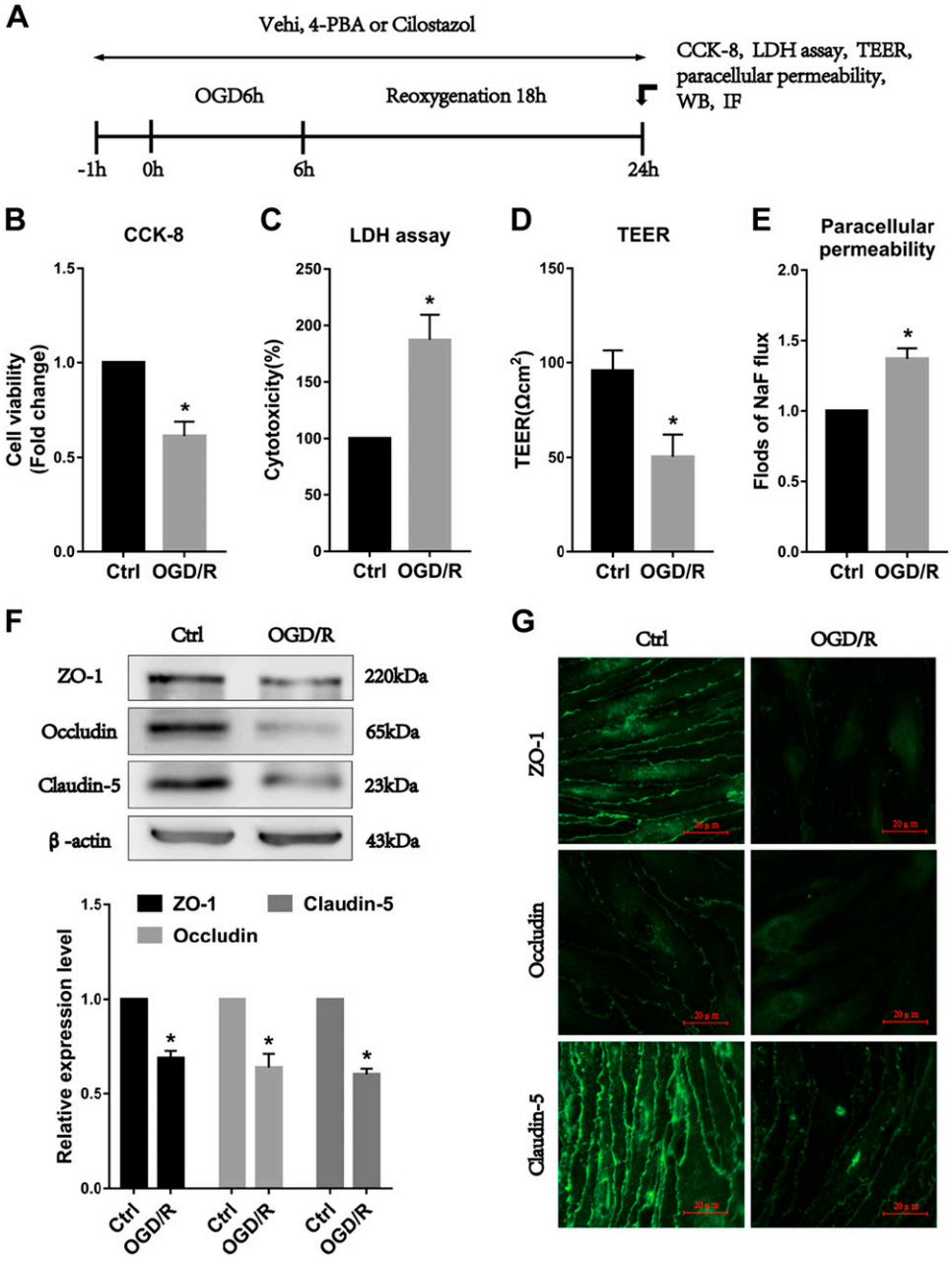


**Figure 1.** OGD/R induced BMVEC injury and reduced TJ protein levels. *A*) Experimental timeline of *in vitro* study. *B, C*) CCK-8 (*B*) assay and LDH (*C*) in bEnd.3 control cells and cells exposed to OGD/R. *D, E*) TEER (*D*) and paracellular permeability determined by Na-F flux (*E*) in control cells and cells exposed to OGD/R. *F, G*) Representative Western blots and their quantifications (*F*) and immunofluorescence staining (*G*) of ZO-1, occludin, and claudin-5 in control cells and cells exposed to OGD/R. Ctrl, control; IF, immunofluorescence; Vehi, vehicle; WB, Western blot; $n \geq 3$ for each group. $^*P < 0.05$ *vs.* control.

## OGD/R-induced ER stress in bEnd.3 cells

To elucidate the role of ER stress in OGD/R-induced cell injury, ER stress–associated protein levels were assessed during the reoxygenation period by collecting cells at various reoxygenation times (0, 2, 4, 6, 12, 18 h) after 6 h of OGD. As shown in **Fig. 2**, cells exposed to reoxygenation after OGD exhibited increased levels of ER stress–related proteins such as p-PERK, p-IRE1-α, ATF-6, and Bip in a time-dependent manner. These results suggest that OGD/R induces ER stress in bEnd.3 cells during reoxygenation.

## Pretreatment with cilostazol and 4-PBA attenuates ER stress induced by OGD/R

To examine the protective effects of the ER stress inhibitors 4-PBA and cilostazol on OGD/R-induced brain endothelial cell injury, bEnd.3 cells were pretreated with vehicle, 4-PBA, or cilostazol for 1 h before and during OGD/R. First, we examined the effects of a series of concentrations of 4-PBA or cilostazol on cell viability (**Fig. 3*A***). Cells were treated with vehicle (0.1% DMSO), 4-PBA (10, 50, 100, 200, 500 μM), or cilostazol (1, 3, 5, 10, 30 μM) during OGD/R, and we found that 100 μM of 4-PBA or 3 μM of cilostazol could optimally reverse OGD/R-induced cytotoxicity, as well as a significant decrease in the release of LDH compared with that for vehicle (Fig. 3*B*); thus, we chose these concentrations for subsequent studies. Next, we examined the effect of 4-PBA or cilostazol on ER stress–related proteins in bEnd.3 cells during early (4 h) reoxygenation periods after 6 h of OGD. After 4 h of reperfusion, ER stress–related proteins were significantly increased compared with those in control cells, and this increase was significantly suppressed by 4-PBA (*vs.* vehicle; Fig. 3*C*). In contrast, the significantly increased

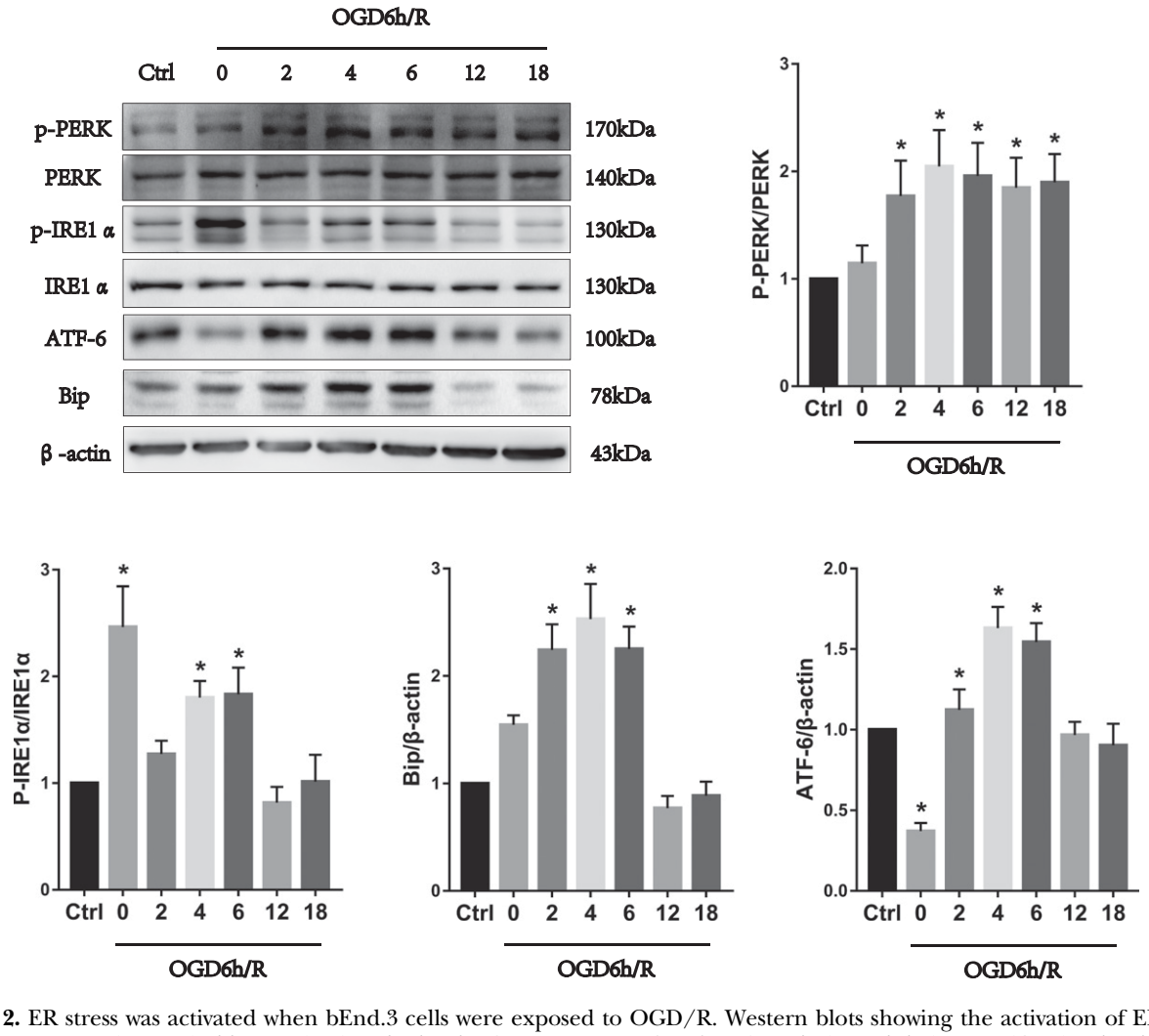


**Figure 2.** ER stress was activated when bEnd.3 cells were exposed to OGD/R. Western blots showing the activation of ER stress during reoxygenation period by monitoring the levels of p-PERK, p-IRE1-α, ATF-6, and Bip and their quantification levels; $n \geq 3$ for each group. *$P<0.05$ *vs.* control.

levels of ER stress–related proteins in vehicle-treated cells were also significantly reduced by pretreatment with cilostazol (*vs.* vehicle; Fig. 3*C*).

## 4-PBA and cilostazol protect brain endothelial TJs from OGD/R

To examine whether the attenuation of ER stress exerts protective effects on OGD/R-induced TJ disruption, endothelial barrier function was tested after OGD/R with or without treatment with 4-PBA or cilostazol. Both 4-PBA or cilostazol significantly attenuated OGD/R-induced changes in paracellular permeability and TEER (**Fig. 4*A*, *B***). We also examined whether levels of the transmembrane proteins ZO-1, occludin, and claudin-5 could be regulated by 4-PBA or cilostazol. The reduction in ZO-1, occludin, and claudin-5 protein levels by OGD/R was significantly prevented by 4-PBA or cilostazol (*vs.* vehicle; Fig. 4*C*). The conservation of TJ proteins with 4-PBA or cilostazol in cells exposed to OGD/R was further supported by immunofluorescence staining for ZO-1, occludin, and claudin-5 (Fig. 4*D*). These results suggest that ER stress mediates the actions of I/R injury in brain endothelial cells. We thus hypothesized that the protective effect of cilostazol on I/R-induced endothelial cell injury might be related to the attenuation of ER stress.

## 4-PBA or cilostazol reverses I/R-induced ER stress and preserves the BBB *in vivo*

To further identify whether ER stress is related to I/R-induced BBB disruption, we used an I/R injury model in rats (**Fig. 5*A***). As illustrated in Fig. 5*B*, intervention with 4-PBA or cilostazol successfully improved neurologic performance after I/R. The permeability to EB was also increased following I/R, a phenomenon that was partially inhibited by 4-PBA or cilostazol (Fig. 5*C*). Western blotting for TJ proteins to analyze the BBB structure was then performed; after I/R, the expression of TJ proteins including ZO-1, occludin, and claudin-5 decreased, and this decrease was partly reversed by the administration of 4-PBA or cilostazol (Fig. 5*D*). Similarly, Western blotting indicated that ER stress was activated after I/R, and treatment with 4-PBA or cilostazol was found to reverse these changes

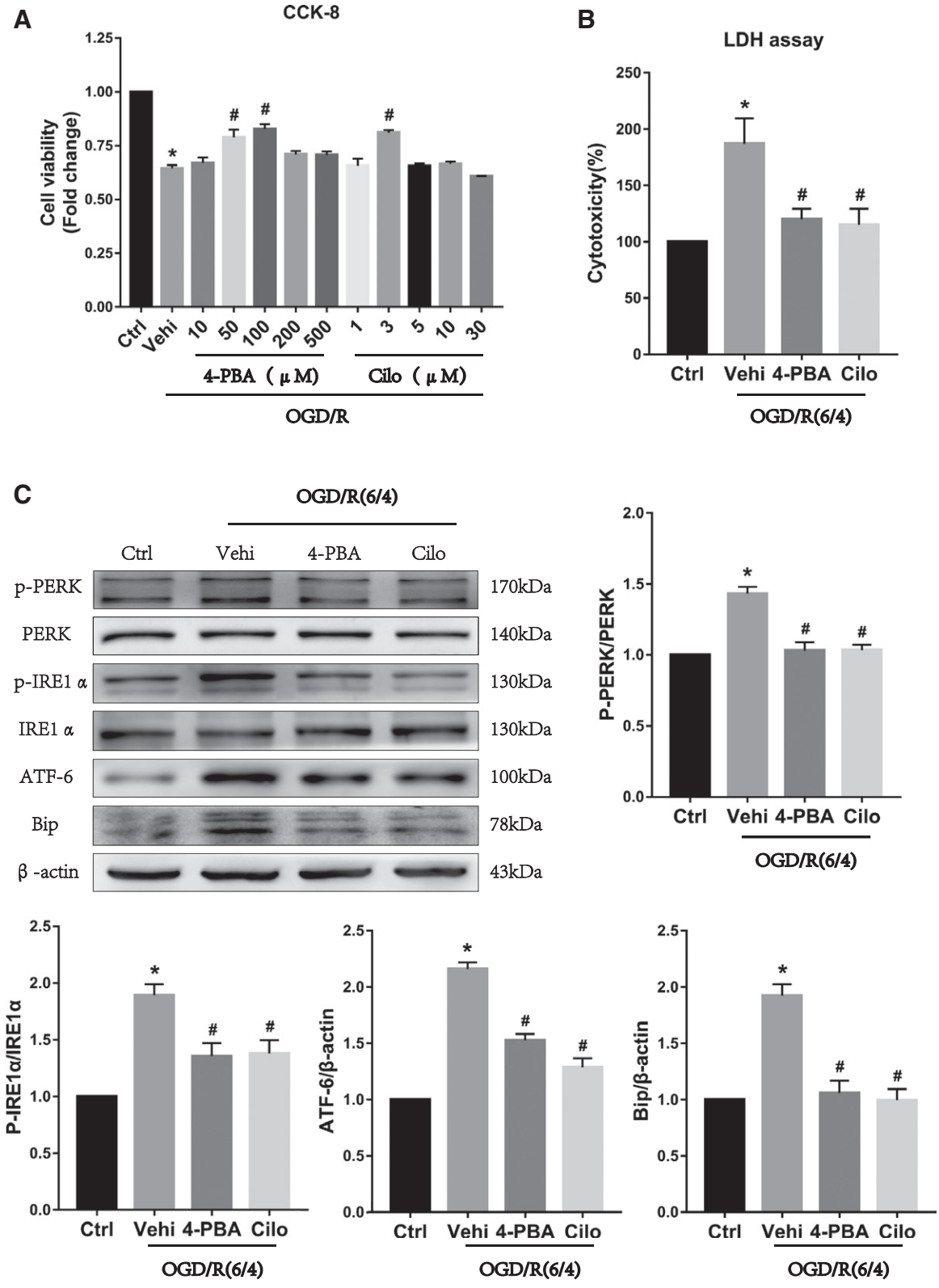


**Figure 3.** Effects of ER stress inhibitor 4-PBA or cilostazol (Cilo) on bEnd.3 exposed to OGD/R. *A*) CCK-8 assay of cells treated with vehicle (Vehi; 0.1% DMSO), 4-PBA (10, 50, 100, 200, 500 μM), or Cilo (1, 3, 5, 10, 30 μM) during OGD/R, and found that 100 μM of 4-PBA or 3 μM of Cilo could significantly reduce cell injury. *B*) LDH assay of cells treated with Vehi (0.1% DMSO), 4-PBA (100 μM), or Cilo (3 μM) during OGD/R. *C*) Representative Western blots of p-PERK, PERK, p-IRE1-α, IRE1-α, ATF-6, Bip proteins and their quantifications in control (Ctrl) and cells treated with Vehi, 4-PBA (100 μM), or Cilo (3 μM) 4 h after OGD (OGD/R); $n \geq 3$ for each group. $^{*}P < 0.05$ *vs.* Ctrl, $^{\#}P < 0.05$ *vs.* Vehi.

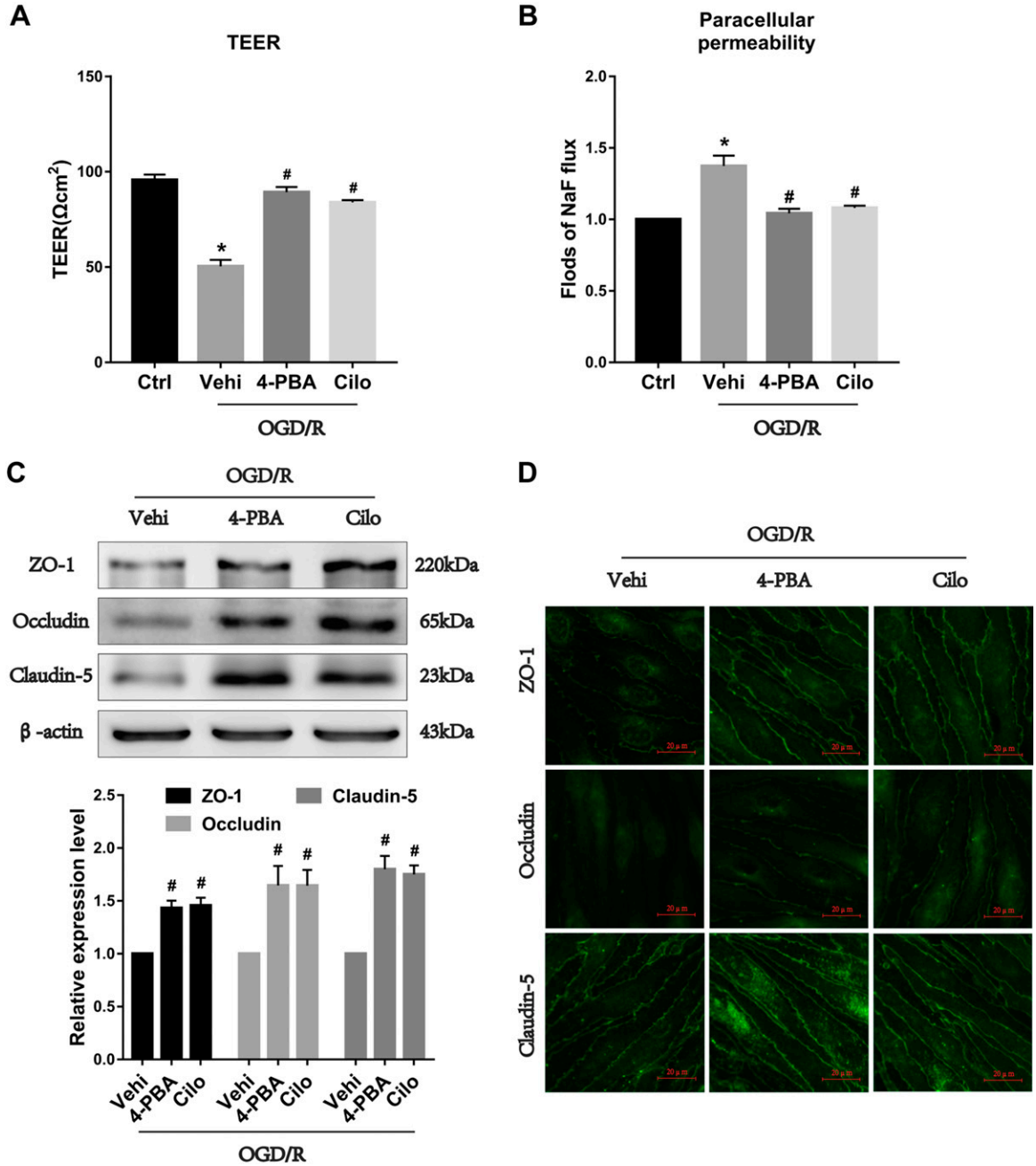


**Figure 4.** Effects of ER stress inhibitor 4-PBA or cilostazol on reduced TJ protein levels in brain endothelial cells after OGD/R (6/4). *A*, *B*) TEER (*A*) and paracellular permeability (*B*) of cells treated with vehicle (Vehi), 4-PBA, or cilostazol (Cilo) during OGD/R. *C*, *D*) Representative Western blots and their quantifications (*C*) and representative immunofluorescence staining (*D*) of ZO-1, occludin, and claudin-5 (green) in OGD/R-exposed cells treated with Vehi, 4-PBA, or Cilo. Ctrl, control; $n \geq 3$ for each group. $^{*}P < 0.05$ *vs.* Ctrl, $^{\#}P < 0.05$ *vs.* Vehi.

(Fig. 5*E*). Together, our results suggest that ER stress is related to the I/R-induced disruption of the BBB *in vivo* and that attenuation of ER stress levels mediated by cilostazol could be a potential strategy to reverse I/R injury.

## OGD/R-induced ER stress is involved in activation of the NF-κB–MMP-9 cascade and MMP-9 secretion

To further elucidate the mechanisms associated with ER stress–induced disruption of TJs, changes in the levels of MMP-9 were tested because this enzyme has been shown to degrade TJ proteins (claudin-5, occludin, and ZO-1) both in cultured brain endothelial cells and in animal models of focal cerebral ischemia. MMP-9 levels in the medium and mRNA levels were examined using bEnd.3 cells during early (4 h) and late (18 h) reperfusion periods after 6 h of OGD. After 4 h of reoxygenation, MMP-9 levels in the medium were slightly increased, whereas at 18 h, MMP-9 levels were further significantly increased compared with those in control cells; furthermore, this increase was significantly reversed by either

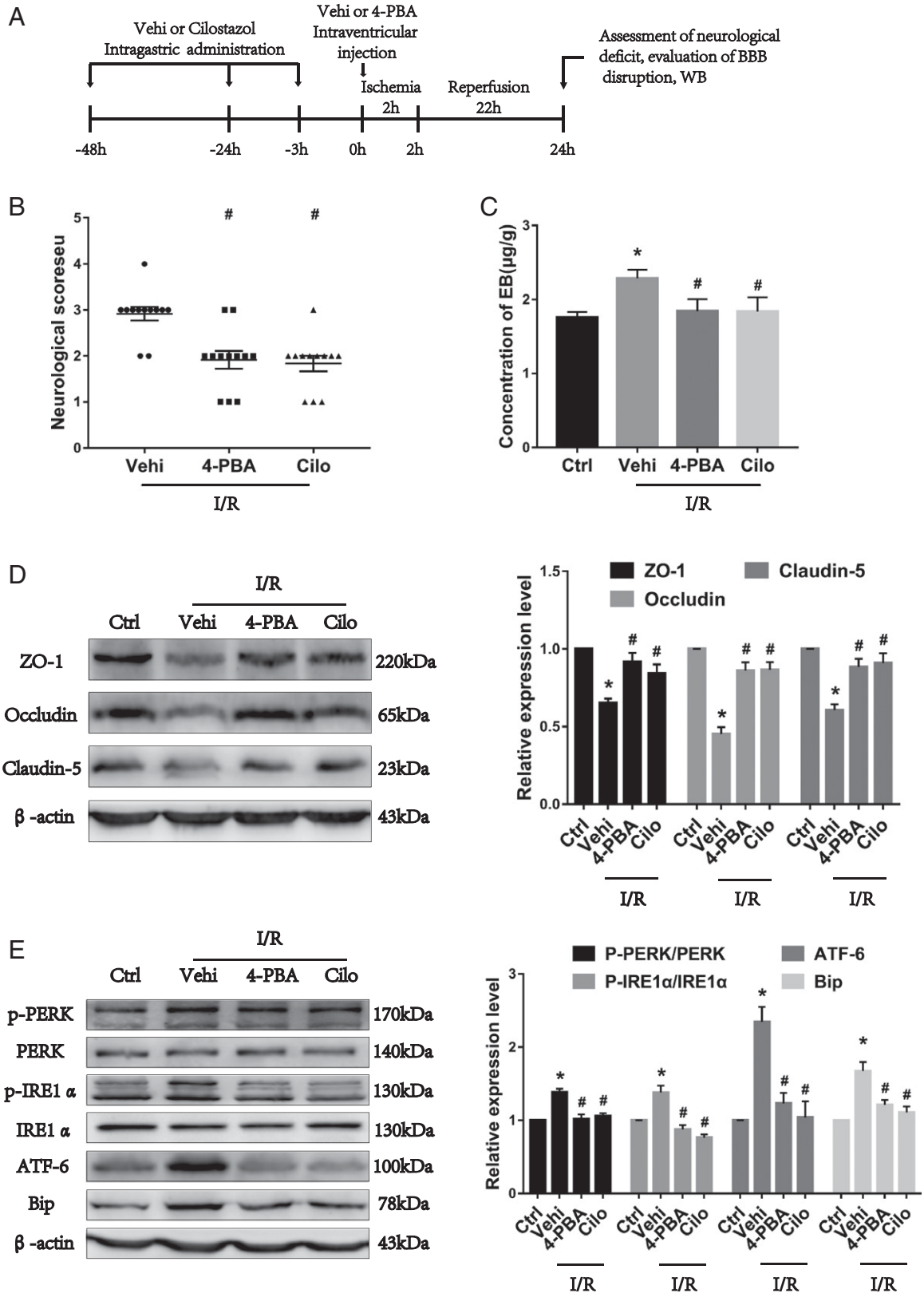


**Figure 5.** 4-PBA or cilostazol (Cilo) partly reversed I/R-induced disruption of the BBB *in vivo*. Rats were randomly divided into 4 experimental groups: control (Ctrl), vehicle (Vehi), 4-PBA, and Cilo. *A*) Experimental timeline of *in vivo* study. *B*) Neurologic scores evaluated after 22 h of reperfusion. *C*) The leakage of EB: EB extravasation in a whole brain and quantification. *D*) Western blot analysis of TJ proteins ZO-1, occludin, and claudin-5 in brain and quantification. *E*) Western blot analysis of ER stress–related proteins p-PERK, p-IRE1-α, ATF-6, Bip proteins in brain and their quantifications; $n = 6$. $^{*}P < 0.05$ *vs.* Ctrl, $^{\#}P < 0.05$ *vs.* Vehi.

4-PBA or cilostazol (**Fig. 6*A***). RT-PCR showed that *MMP-9* mRNA expression was increased in cells treated with OGD/R, and this change was reversed by the administration of 4-PBA or cilostazol (Fig. 6*B*). These data indicate that OGD/R stimulates MMP-9 expression and secretion in endothelial cells, whereas pre-exposure of endothelial cells to 4-PBA or cilostazol can attenuate this.

We next investigated signaling molecules that mediate OGD/R-induced MMP-9 expression. Because it has been reported that NF-κB is the major transcription factor that induces the expression of MMP-9, experiments were carried out to determine whether OGD/R-induced ER stress is associated with regulation of the NF-κB pathway. Western blotting suggested that OGD/R induces the up-regulation of nuclear p-NF-κB, both in the early and late stages of reoxygenation; moreover, these increases were successfully altered by 4-PBA or cilostazol treatment (Fig. 6*C*).

## DISCUSSION

The leakage of blood *via* disruption of the BBB plays an important role in HT. However, despite its clinical significance, no effective treatment for HT has been identified. The BBB comprises a layer of tightly connected BMVECs that interact with other brain cells including astrocytes, neurons, and pericytes (15). The bEnd.3 cells used in this study are mouse-derived BMVECs and are well accepted as an *in vitro* model for BBB investigations (16). In the present study, we performed OGD/R using bEnd.3 cells to mimic I/R injury *in vitro*, together with an *in vivo* I/R model.

In our current study, we made the following observations: *1*) OGD/R induced brain endothelial cell injury and TJ disruption, accompanied by the activation of ER stress; *2*) ER stress was involved in the disruption of TJs after OGD/R, and the protective effect of cilostazol involved inhibiting ER stress after OGD/R; *3*) inhibition of ER stress might prevent BBB damage by suppressing the up-regulation and translocation of NF-κB and reducing the expression and secretion of MMP-9. Taken together, our results provide evidence that BBB damage is reduced by inhibiting the activation of ER stress during cerebral I/R.

First, we tested whether the conditions used in this study could mimic I/R injury–induced BBB disruption. OGD for 6 h followed by 18 h of reoxygenation inhibited the viability of bEnd.3 cells and reduced the expression of TJs, resulting in reduced endothelial barrier integrity, decreased TEER, and increased paracellular permeability. Moreover, during the reoxygenation period, ER stress was activated. Ischemia-induced energy depletion rapidly disrupts ER calcium homeostasis and subsequently impairs protein folding, which ultimately can lead to cell death (17). Even during reperfusion, ER stress–related protein levels were continuously elevated, suggesting the persistent activation of ER stress. To our knowledge, studies on I/R-induced ER stress in the brain have focused mainly on neuronal cells (18–20) and astrocytes (21, 22) *in vitro* and *in vivo*. To date, the mechanisms responsible for ER stress associated with I/R-induced BBB disruption have remained unclear. Chen *et al.* (23) reported that the activation of ER stress induced by A-$\beta_{1-42}$ disrupts the TJs of bEnd.3 cells in a receptor for advanced glycation end products–dependent manner. In addition, activation of ER stress mediated by methamphetamine was found to disrupt BBBs and induce endothelial cell damage, which further induced mitochondrial dysfunction, and it was found that 4-PBA could be an effective treatment for methamphetamine-induced BBB disruption (24). The activation of ER stress induced by diabetes exacerbates the disruption of blood–spinal cord barrier after spinal cord injury, and inhibition of ER stress by 4-PBA might have a beneficial effect on the integrity of the blood–spinal cord barrier in diabetic spinal cord injury rats, leading to improved recovery (25). However, studies on ER stress–related endothelial cell injury after I/R are limited. Having observed the relevance of ER stress with respect to I/R injury, we postulated that the inhibition of this response might be protective against I/R-induced cerebral injury. To corroborate this hypothesis, 4-PBA, a chemical chaperone, was selected as an ER stress inhibitor and administered concurrently with ischemic exposure and reperfusion. 4-PBA is a Food and Drug Administration–approved drug used for children with urea cycle disorders (26). Furthermore, it was reported to protect against ischemic brain injury by inhibiting ER stress–mediated apoptosis and inflammation (27). The dose of this drug used in this study was in accordance with the dose-effect relationship between 4-PBA and OGD/R based on cell viability assessments using CCK-8 *in vitro* and *in vivo* performed in other studies (28). In the present study, this ER stress inhibitor prevented OGD/R-induced endothelial cell injury and TJ disruption with changes to paracellular permeability, TEER, and TJ protein levels *in vitro*. Furthermore, results were consistent with an *in vivo* study, indicating that ER stress mediates I/R injury in endothelial cells.

Our study also showed that the protective effects of ER stress inhibition on TJ protein levels are associated with the inhibition of NF-κB–MMP-9 activation during the reperfusion period. To our knowledge, this is the first study to demonstrate that the inhibition of ER stress after I/R is involved in the protective effects against TJ disruption by inhibiting signaling molecules activated by ischemic insult. Among several signaling molecules that affect TJ protein levels, we focused on NF-κB–MMP-9 because these molecules are associated with ischemia-induced disruption of the BBB. MMP-9 has been shown to degrade TJ proteins (claudin-5, occludin, and ZO-1) in cultured brain endothelial cells and in animal models of focal cerebral ischemia (29, 30). High-plasma MMP-9 concentrations during the acute phase of cerebral infarction are considered an independent predictor of HT in stroke patients (31, 32). Experimental data indicate that, except for infiltrating leukocytes (often

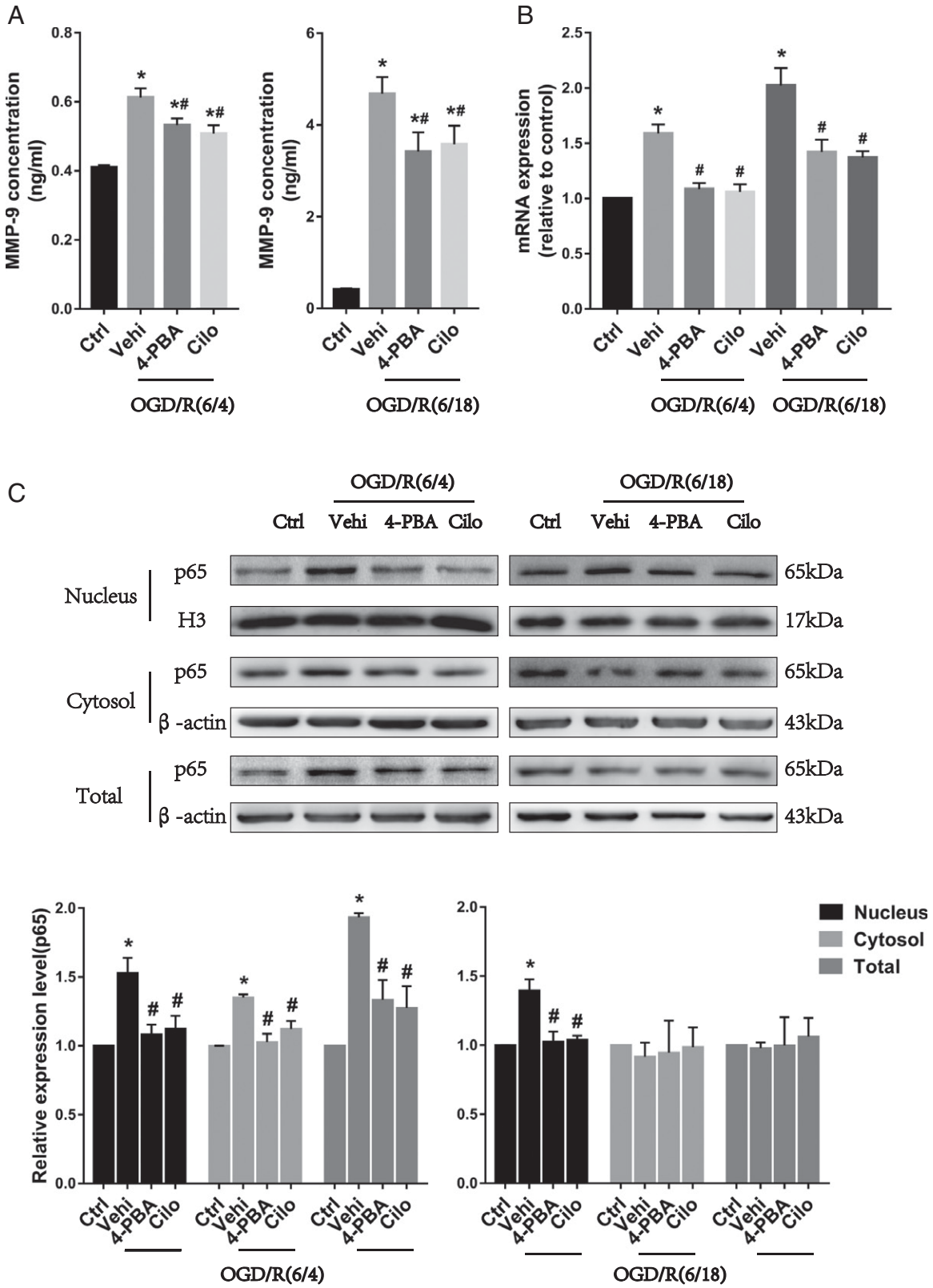


**Figure 6.** OGD/R-induced ER stress is involved in activation of NF-kB–MMP-9 cascade and MMP-9 secretion. *A*) Quantification results of the MMP-9 levels in the culture medium. *B*) RT-PCR quantification results of MMP-9 mRNA expressions in control cells (Ctrl) and cells treated with vehicle (Vehi), 4-PBA, or cilostazol (Cilo) 4 and 18 h after OGD (OGD/R). *C*) Western blot analysis of p-NF-kB (p65) both in nucleus and cytosol and total protein level and their quantifications; $n \geq 3$ for each group. $^{*}P < 0.05$ *vs.* Ctrl, $^{\#}P < 0.05$ *vs.* Vehi.

neutrophils), BMVECs are key cellular indicators of brain MMP-9, at least during the early phase after focal cerebral ischemia (30, 33). Similarly, in the present study, we found that OGD/R stimulates MMP-9 expression and secretion in endothelial cells, whereas inhibition of ER stress reverses these changes. The translocation of NF-κB, which is the major transcription factor that regulates MMP-9 expression, to the nuclei was observed after OGD/R, and this change was reversed by inhibiting ER stress. Meanwhile, translocation of ATF-6 was reported to participate in the regulation of the NF-κB pathway, probably by up-regulating the transcription of genes that activate this pathway (34). Therefore, our data demonstrate that ER stress might modulate the activation of the NF-κB–MMP-9 cascade and MMP-9 secretion.

It was reported that cilostazol has protective effects on vascular endothelial cells (12–14). In addition, increasing evidence has shown that cilostazol also exerts a protective effect by promoting BBB integrity (35, 36). Therefore, it is necessary to evaluate the benefits of preischemia cilostazol administration and the underlying molecular mechanisms. Concerning the BBB and the protective effects of cilostazol on I/R, we suppose that this might be related to the attenuation of ER stress.

In the present study, we further studied the role of cilostazol in protection against I/R-induced BBB injury and its mechanisms. We found that pretreating cells with 3 μM of cilostazol could optimally reverse OGD/R-induced cytotoxicity. The concentrations of cilostazol (3 μM) that we used in this study were similar to serum concentrations found to have clinical utility (37). Similar to effects observed with an ER stress inhibitor, the administration of cilostazol prevented OGD/R-induced endothelial cell injury and TJ disruption, with changes in paracellular permeability, TEER, and TJ protein levels *in vitro*, which was also observed *in vivo*. Meanwhile, activated ER stress was reversed, and subsequently, the translocation of NF-κB was reduced, and MMP-9 expression and secretion into the medium were attenuated during reoxygenation after OGD for 6 h. Therefore, cilostazol exerts its protective effects against BBB injury after I/R at least in part by inhibiting ER stress. Cilostazol could increase the intracellular level of cAMP by inhibiting its hydrolysis by type III phosphodiesterase. Decreasing adenylate cyclase activity and intracellular cAMP levels after hypoxia is associated with impaired endothelial barrier function, which may contribute to increased vascular permeability (38). The cAMP levels in our *in vitro* model were tested. As shown in Supplemental Fig. S1, in an untreated control group, cAMP levels were significantly elevated following treatment with cilostazol. Following 6 h of OGD, the cAMP levels underwent a substantial down-regulation after hypoxia, then increased in a time-dependent manner before returning to

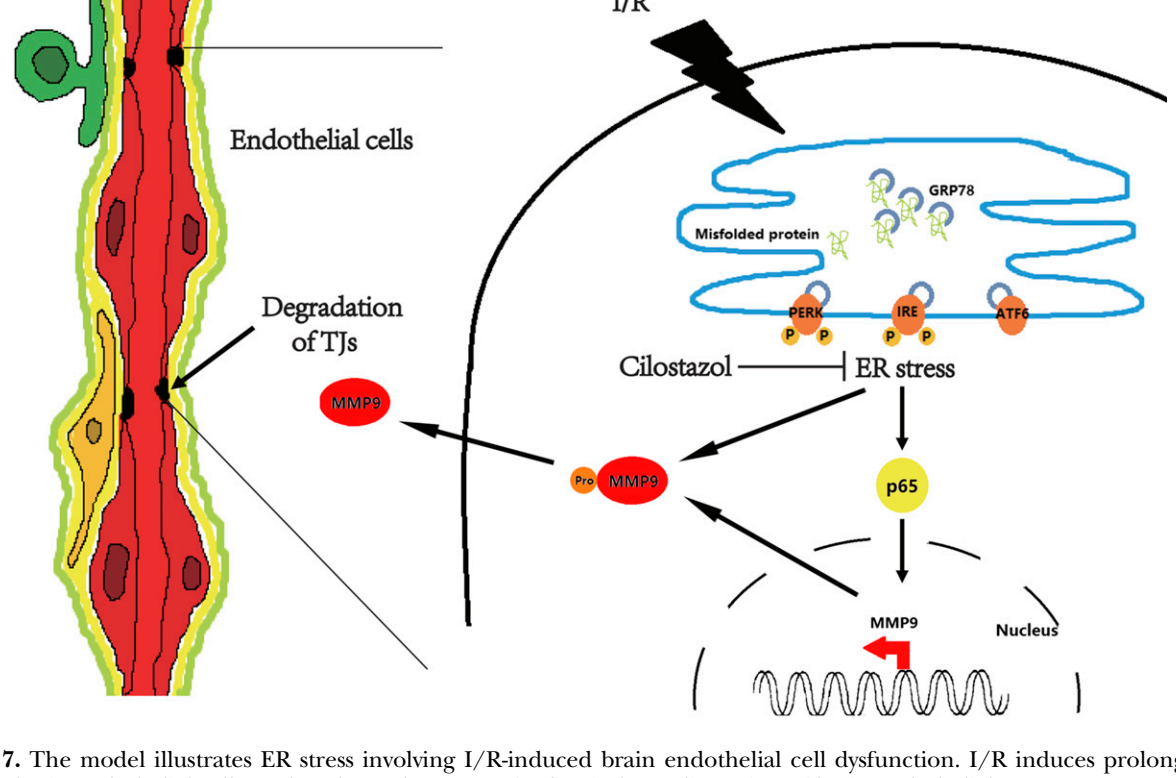


**Figure 7.** The model illustrates ER stress involving I/R-induced brain endothelial cell dysfunction. I/R induces prolonged ER stress in brain endothelial cells, and prolonged ER stress further induces disruption of brain endothelial TJ. ER stress may induce activation of NF-kB–MMP-9 cascade and secretion of MMP-9, which participates in disruption of TJs. Cilostazol ameliorates I/R-induced brain endothelial TJ injury by inhibiting ER stress activation.

near normal levels during reoxygenation. These changes can be reversed by treatment with cilostazol but not ER stress inhibitor. Although it has been proposed that treatment with 4-PBA attenuates the ER stress response and rescued cAMP accumulation deficiency in DYT1 (hereditary dystonia caused by mutation in the TOR1A gene) patient fibroblast lines comparable to control fibroblast cAMP levels (39), our results present no change in cAMP levels after treatment with 4-PBA in our model. This may be because the concentration of 4-PBA they used in their experiment was much higher (5 mM) than that in our experiment (100 μM). Accordingly, these results indicate that there might exist other mechanisms with a protective effect on BBB disruption of cilostazol other than the inhibition of type III phosphodiesterase.

In summary, as illustrated in **Fig. 7**, we demonstrate that ER stress is activated after transient ischemic stroke and has a deleterious role in BBB integrity. Therefore, ER stress could be a potential therapeutic target to mitigate BBB disruption after I/R. Cilostazol appears to improve I/R injury by inhibiting the disruption of TJ proteins and suppressing ER stress and thus might be a promising therapeutic agent to protect against BBB damage after acute ischemic stroke. These findings might provide new ideas to therapeutically protect the BBB from ischemic damage and to extend the window of thrombolysis and reduce cerebral hemorrhage. FJ

## ACKNOWLEDGMENTS

This work was supported by grants from the National Natural Science Foundation of China (81400941) and Neurovascular Disease Discovery Laboratory (NDDL), Beijing (BZ0250). The authors declare no conflicts of interest.

## AUTHOR CONTRIBUTIONS

D. Nan performed experiments, analyzed and interpreted data, and wrote the manuscript; H. Jin, J. Deng, W. Yu, R. Liu, and W. Sun interpreted data and aided in the preparation of the manuscript; Y. Huang supervised the study and provided financial support; and all authors revised the manuscript and approved its final version.

## REFERENCES

1. Strong, K., Mathers, C., and Bonita, R. (2007) Preventing stroke: saving lives around the world. *Lancet Neurol.* **6**, 182–187
2. Goyal, M., Demchuk, A. M., Menon, B. K., Eesa, M., Rempel, J. L., Thornton, J., Roy, D., Jovin, T. G., Willinsky, R. A., Sapkota, B. L., Dowlatshahi, D., Frei, D. F., Kamal, N. R., Montanera, W. J., Poppe, A. Y., Ryckborst, K. J., Silver, F. L., Shuaib, A., Tampieri, D., Williams, D., Bang, O. Y., Baxter, B. W., Burns, P. A., Choe, H., Heo, J. H., Holmstedt, C. A., Jankowitz, B., Kelly, M., Linares, G., Mandzia, J. L., Shankar, J., Sohn, S. I., Swartz, R. H., Barber, P. A., Coutts, S. B., Smith, E. E., Morrish, W. F., Weill, A., Subramaniam, S., Mitha, A. P., Wong, J. H., Lowerison, M. W., Sajobi, T. T., and Hill, M. D.; ESCAPE Trial Investigators. (2015) Randomized assessment of rapid endovascular treatment of ischemic stroke. *N. Engl. J. Med.* **372**, 1019–1030
3. Duehrkop, C., and Rieben, R. (2014) Ischemia/reperfusion injury: effect of simultaneous inhibition of plasma cascade systems versus specific complement inhibition. *Biochem. Pharmacol.* **88**, 12–22
4. Pan, J., Konstas, A. A., Bateman, B., Ortolano, G. A., and Pile-Spellman, J. (2007) Reperfusion injury following cerebral ischemia: pathophysiology, MR imaging, and potential therapies. *Neuroradiology* **49**, 93–102
5. Xin, Q., Ji, B., Cheng, B., Wang, C., Liu, H., Chen, X., Chen, J., and Bai, B. (2014) Endoplasmic reticulum stress in cerebral ischemia. *Neurochem. Int.* **68**, 18–27
6. Walter, P., and Ron, D. (2011) The unfolded protein response: from stress pathway to homeostatic regulation. *Science* **334**, 1081–1086
7. Tabas, I., and Ron, D. (2011) Integrating the mechanisms of apoptosis induced by endoplasmic reticulum stress. *Nat. Cell Biol.* **13**, 184–190
8. Chen, X., Kintner, D. B., Luo, J., Baba, A., Matsuda, T., and Sun, D. (2008) Endoplasmic reticulum Ca2+ dysregulation and endoplasmic reticulum stress following *in vitro* neuronal ischemia: role of Na+-K+-Cl- cotransporter. *J. Neurochem.* **106**, 1563–1576
9. Paschen, W., and Doutheil, J. (1999) Disturbances of the functioning of endoplasmic reticulum: a key mechanism underlying neuronal cell injury? *J. Cereb. Blood Flow Metab.* **19**, 1–18
10. Schinzel, A. C., Takeuchi, O., Huang, Z., Fisher, J. K., Zhou, Z., Rubens, J., Hetz, C., Danial, N. N., Moskowitz, M. A., and Korsmeyer, S. J. (2005) Cyclophilin D is a component of mitochondrial permeability transition and mediates neuronal cell death after focal cerebral ischemia. *Proc. Natl. Acad. Sci. USA* **102**, 12005–12010
11. Tanaka, Y., Tanaka, R., Liu, M., Hattori, N., and Urabe, T. (2010) cilostazol attenuates ischemic brain injury and enhances neurogenesis in the subventricular zone of adult mice after transient focal cerebral ischemia. *Neuroscience* **171**, 1367–1376
12. Nonaka, Y., Tsuruma, K., Shimazawa, M., Yoshimura, S., Iwama, T., and Hara, H. (2009) cilostazol protects against hemorrhagic transformation in mice transient focal cerebral ischemia-induced brain damage. *Neurosci. Lett.* **452**, 156–161
13. Ishiguro, M., Suzuki, Y., Mishiro, K., Kakino, M., Tsuruma, K., Shimazawa, M., Yoshimura, S., Iwama, T., and Hara, H. (2011) Blockade of phosphodiesterase-III protects against oxygen-glucose deprivation in endothelial cells by upregulation of VE-cadherin. *Curr. Neurovasc. Res.* **8**, 86–94
14. Kim, K. Y., Shin, H. K., Choi, J. M., and Hong, K. W. (2002) Inhibition of lipopolysaccharide-induced apoptosis by cilostazol in human umbilical vein endothelial cells. *J. Pharmacol. Exp. Ther.* **300**, 709–715
15. Tajes, M., Ramos-Fernández, E., Weng-Jiang, X., Bosch-Morató, M., Guivernau, B., Eraso-Pichot, A., Salvador, B., Fernàndez-Busquets, X., Roquer, J., and Muñoz, F. J. (2014) The blood-brain barrier: structure, function and therapeutic approaches to cross it. *Mol. Membr. Biol.* **31**, 152–167
16. Watanabe, T., Dohgu, S., Takata, F., Nishioku, T., Nakashima, A., Futagami, K., Yamauchi, A., and Kataoka, Y. (2013) Paracellular barrier and tight junction protein expression in the immortalized brain endothelial cell lines bEND.3, bEND.5 and mouse brain endothelial cell 4. *Biol. Pharm. Bull.* **36**, 492–495
17. Szydlowska, K., and Tymianski, M. (2010) Calcium, ischemia and excitotoxicity. *Cell Calcium* **47**, 122–129
18. DeGracia, D. J., and Montie, H. L. (2004) Cerebral ischemia and the unfolded protein response. *J. Neurochem.* **91**, 1–8
19. Tajiri, S., Oyadomari, S., Yano, S., Morioka, M., Gotoh, T., Hamada, J. I., Ushio, Y., and Mori, M. (2004) Ischemia-induced neuronal cell death is mediated by the endoplasmic reticulum stress pathway involving CHOP. *Cell Death Differ.* **11**, 403–415
20. Paschen, W., and Mengesdorf, T. (2005) Cellular abnormalities linked to endoplasmic reticulum dysfunction in cerebrovascular disease–therapeutic potential. *Pharmacol. Ther.* **108**, 362–375
21. Shu, Q., Fan, H., Li, S. J., Zhou, D., Ma, W., Zhao, X. Y., Yan, J. Q., and Wu, G. (2018) Protective effects of Progranulin against focal cerebral ischemia-reperfusion injury in rats by suppressing endoplasmic reticulum stress and NF-κB activation in reactive astrocytes. *J. Cell. Biochem.* **119**, 6584–6597
22. Yu, Z., Yi, M., Wei, T., Gao, X., and Chen, H. (2017) KCa3.1 inhibition switches the astrocyte phenotype during astrogliosis associated with ischemic stroke via endoplasmic reticulum stress and MAPK signaling pathways. *Front. Cell. Neurosci.* **11**, 319
23. Chen, W., Chan, Y., Wan, W., Li, Y., and Zhang, C. (2018) $A\beta_{1\text{-}42}$ induces cell damage via RAGE-dependent endoplasmic reticulum stress in bEnd.3 cells. *Exp. Cell Res.* **362**, 83–89

24. Qie, X., Wen, D., Guo, H., Xu, G., Liu, S., Shen, Q., Liu, Y., Zhang, W., Cong, B., and Ma, C. (2017) Endoplasmic reticulum stress mediates methamphetamine-induced blood-brain barrier damage. *Front. Pharmacol.* **8**, 639
25. He, Z., Zou, S., Yin, J., Gao, Z., Liu, Y., Wu, Y., He, H., Zhou, Y., Wang, Q., Li, J., Wu, F., Xu, H. Z., Jia, X., and Xiao, J. (2017) Inhibition of endoplasmic reticulum stress preserves the integrity of blood-spinal cord barrier in diabetic rats subjected to spinal cord injury. *Sci. Rep.* **7**, 7661
26. Maestri, N. E., Brusilow, S. W., Clissold, D. B., and Bassett, S. S. (1996) Long-term treatment of girls with ornithine transcarbamylase deficiency. *N. Engl. J. Med.* **335**, 855–859
27. Qi, X., Hosoi, T., Okuma, Y., Kaneko, M., and Nomura, Y. (2004) Sodium 4-phenylbutyrate protects against cerebral ischemic injury. *Mol. Pharmacol.* **66**, 899–908
28. Feng, D., Wang, B., Wang, L., Abraham, N., Tao, K., Huang, L., Shi, W., Dong, Y., and Qu, Y. (2017) Pre-ischemia melatonin treatment alleviated acute neuronal injury after ischemic stroke by inhibiting endoplasmic reticulum stress-dependent autophagy via PERK and IRE1 signalings. *J. Pineal Res.* **62**, e12395
29. Yang, Y., Estrada, E. Y., Thompson, J. F., Liu, W., and Rosenberg, G. A. (2007) Matrix metalloproteinase-mediated disruption of tight junction proteins in cerebral vessels is reversed by synthetic matrix metalloproteinase inhibitor in focal ischemia in rat. *J. Cereb. Blood Flow Metab.* **27**, 697–709
30. McColl, B. W., Rothwell, N. J., and Allan, S. M. (2008) Systemic inflammation alters the kinetics of cerebrovascular tight junction disruption after experimental stroke in mice. *J. Neurosci.* **28**, 9451–9462
31. Planas, A. M., Solé, S., and Justicia, C. (2001) Expression and activation of matrix metalloproteinase-2 and -9 in rat brain after transient focal cerebral ischemia. *Neurobiol. Dis.* **8**, 834–846
32. Castellanos, M., Leira, R., Serena, J., Pumar, J. M., Lizasoain, I., Castillo, J., and Dávalos, A. (2003) Plasma metalloproteinase-9 concentration predicts hemorrhagic transformation in acute ischemic stroke. *Stroke* **34**, 40–46
33. Jin, R., Yang, G., and Li, G. (2010) Inflammatory mechanisms in ischemic stroke: role of inflammatory cells. *J. Leukoc. Biol.* **87**, 779–789
34. Yamazaki, H., Hiramatsu, N., Hayakawa, K., Tagawa, Y., Okamura, M., Ogata, R., Huang, T., Nakajima, S., Yao, J., Paton, A. W., Paton, J. C., and Kitamura, M. (2009) Activation of the Akt-NF-kappaB pathway by subtilase cytotoxin through the ATF6 branch of the unfolded protein response. *J. Immunol.* **183**, 1480–1487
35. Horai, S., Nakagawa, S., Tanaka, K., Morofuji, Y., Couraud, P. O., Deli, M. A., Ozawa, M., and Niwa, M. (2013) cilostazol strengthens barrier integrity in brain endothelial cells. *Cell. Mol. Neurobiol.* **33**, 291–307
36. Torii, H., Kubota, H., Ishihara, H., and Suzuki, M. (2007) cilostazol inhibits the redistribution of the actin cytoskeleton and junctional proteins on the blood-brain barrier under hypoxia/reoxygenation. *Pharmacol. Res.* **55**, 104–110
37. Akiyama, H., Kudo, S., and Shimizu, T. (1985) The metabolism of a new antithrombotic and vasodilating agent, cilostazol, in rat, dog and man. *Arzneimittelforschung* **35**(7A), 1133–1140
38. Deli, M. A., Abrahám, C. S., Kataoka, Y., and Niwa, M. (2005) Permeability studies on *in vitro* blood-brain barrier models: physiology, pathology, and pharmacology. *Cell. Mol. Neurobiol.* **25**, 59–127
39. Cho, J. A., Zhang, X., Miller, G. M., Lencer, W. I., and Nery, F. C. (2014) 4-Phenylbutyrate attenuates the ER stress response and cyclic AMP accumulation in DYT1 dystonia cell models. *PLoS One* **9**, e110086

*Received for publication February 1, 2019.*
*Accepted for publication May 13, 2019.*